GLASS-CERAMIC X-RAY AND THERMAL NEUTRON IMAGING PLATES

G. V. M. Williams[1], A. Edgar[2], G. A. Appleby[2]

[1]MacDiarmid Institute, Industrial Research Limited, P.O. Box 31310, Lower Hutt, New Zealand
[2] MacDiarmid Institute, Victoria University, P.O. Box 600, Wellington, New Zealand

Abstract

We report the results of spatial resolution and conversion efficiency measurements on new fluorochlorozirconate and lithium-borate glass-ceramics that are being researched for x-ray and thermal neutron imaging applications. The sensitivity of the fluorochlorozirconate glass-ceramics containing $BaCl_2:Eu^{2+}$ nano-crystallites is up to 80 % of that found in BaFBr(1000ppm Eu^{2+}), which is the material used in commercial powdered phosphor/polymer x-ray imaging plates. The spatial resolution corresponds to 90 lp/mm and it is much greater than that used in medical imaging plates (e.g. ~2.5 lp/mm for Agfa MD-30). A ^{10}B enriched lithium-borate glass with $BaCl_2:Eu^{2+}$ nano-crystallites had a sensitivity to thermal neutrons that is 145 % of that measured in a commercial thermal neutron imaging plate (Fuji BAS-ND) and the residual radiation can be greatly reduced. The spatial resolution can be improved by selecting nano-crystallites with reduced afterglow.

1. Introduction

X-ray imaging plates based on powdered $BaFBr:Eu^{2+}$ in a polymer binder are replacing photographic film for medical imaging and non-destructive testing applications because of the superior dynamic range, lower dose and the ability to quickly obtain a digital image for later processing. However, they do have a lower spatial resolution (greater than ~100 μm). This is due to light scattering from the $BaFBr:Eu^{2+}$ crystallites.

The mechanism of image generation in polymer/$BaFBr:Eu^{2+}$ imaging plates starts with the incident x-rays exciting electrons and holes that become trapped at defect or impurity sites. The spatial distribution of the trapped electrons and holes represents a latent image. At a later time the plate is illuminated with stimulating light that excites the trapped electrons and holes and leads to recombination and light emission at a different wavelength. The emitted light is detected and the spatial distribution in the light intensity provides an image of the object being x-rayed.

Thermal neutron imaging plates have also been developed because thermal neutrons have a high sensitivity to compounds with low atomic number, which can be compared with x-rays that are more sensitive to compounds with high atomic numbers.

Fujifilm have a BAS-ND thermal neutron imaging plate containing a mixture of powdered Gd_2O_3 and $BaFBr:Eu^{2+}$ (0.1 %) in a polymer binder on a supporting layer. The thermal neutrons are captured by Gd and the reaction products are high energy γ-rays and conversion electrons with energies extending up to 250 keV. The conversion electrons are detected in the powdered $BaFBr:Eu^{2+}$ phosphor and leads to electron-hole pairs that become localized at defect and impurity sites. The read-out method is similar to that for x-ray imaging plates. The γ-ray sensitivity is high in this imaging plate because of the high atomic number elements Gd and Ba. There is also residual radioactivity from thermal neutron capture by ^{79}Br, ^{81}Br and ^{151}Eu. Furthermore, the spatial resolution is limited by scattering and the range of the conversion electrons (tens of μm).

There is clearly an opportunity to develop new x-ray and thermal neutron imaging plates. We have developed a number of glass-ceramics [1-5] and in this paper we report the results from x-ray and thermal neutron spatial resolution and conversion efficiency measurements on two of our glass-ceramics.

2. Experimental details

The fluorochlorozirconate glass-ceramics used in this study are based on a modified ZBLAN20 mix. The preparation of the ZBLAN glasses containing $BaCl_2:Eu^{2+}$ are described elsewhere [4]. X-ray diffraction (XRD) measurements were made on all samples. The as-made glasses were transparent and did not contain any crystallites. They were annealed at temperatures up to 295 °C for up to 12 hours to create the ZBLAN/$BaCl_2:Eu^{2+}$ glass-ceramic containing orthorhombic $BaCl_2:Eu^{2+}$. The crystallite sizes were up to ~100 nm in diameter as estimated

from transmission electron microscope measurements and the XRD linewidths using the Scherrer formula.

Spatial resolution measurements were made on the fluorochlorozirconate glass-ceramics using a Jobin-Yvon confocal micro-Raman spectrometer and a He-Ne laser. A ~130 μm gold foil mask was placed over the sample and it was then x-ray irradiated using a W tube at 50 kV and 20 mA. A focused laser spot (633 nm) was scanned across an edge of the x-ray image and the optically stimulated luminescence (OSL) emission (402 nm) was detected. The laser spot size diameter was less than 1 μm and the detected diameter was ~3.6 μm. The conversion efficiency (CE) was measured after x-ray irradiating by stimulating at 633 nm and time-integrating the OSL emission at wavelengths between 402 nm with a 10 nm bandpass. The CE was referenced to a BaFBr(1000ppm Eu^{2+}) single crystal.

The lithium-borate glass-ceramic for the current study was made from $56.7B_2O_3$-$28.3Li_2O$-$15BaCl_2$ with 99 % ^{10}B enrichment [5]. It was doped with Eu^{2+} as a luminescence centre in the form of $EuCl_2$ (0.5 mol%) and also contained a small amount of SiO_2 to reduce hygroscopy. A previous study has shown that fluoride-doping in halide storage phosphors enhances OSL significantly, so in these materials a small amount of Li_2O was replaced with 2LiF to enhance the PSL. The B_2O_3 was dried at 500 ^oC for one hour in a Pt crucible in an Ar atmosphere. The remaining powders were added in a N_2 atmosphere and melted at 1000 ^oC for one hour in Ar. The melt was poured onto a Cu quenching block held at 300 ^oC, flattened under a second quenching block and cooled slowly to room temperature. Samples of the resulting glassy disc were subsequently annealed at 480 to 540 ^oC to promote crystal growth. Small glass-ceramic neutron imaging plates of size 20 x 20 mm were prepared by lapping the annealed glass-ceramics to a thickness of 0.5 mm (the same thickness as the BAS-ND) and optically polishing one surface.

Each lithium-borate glass-ceramic sample was characterized by XRD and the mean particle size was estimated from the XRD line widths using the Scherrer formula.

A Perkin-Elmer LS-55 luminescence spectrometer was used to measure the photoluminescence (PL) and OSL spectra of each sample. For low energy x-ray induced OSL measurements, samples were irradiated for 30 s with x-rays at room temperature using a Philips PW1720 x-ray generator with W tube operated at 50 kV and 20 mA and filtered through 2 mm of aluminum. The CE was measured using a custom-made OSL detector.

Thermal neutron irradiation was performed at the thermal beam line 32 of the spallation neutron source SINQ, which is known as the NEUTRA facility at the Paul Scherrer Institute, Switzerland. The neutron flux was 4.75×10^6 n cm^{-2} s^{-1} of polychromatic neutrons with a thermal Maxwellian energy spectrum and most probable energy at 23 meV. Samples were irradiated from 2 to 45 s using a variety of imaging objects and the images were read out using a BAS2500 Imaging Plate readout scanner produced by Fujifilm. The images made were compared to those obtained using Fujifilm's commercial BAS-ND thermal neutron imaging plate.

3. Results and analysis

The maximum CE of the ZBLAN/$BaCl_2$:Eu^{2+} glass ceramics was estimated to be 80 % relative to a BaFBr:(1000ppm Eu^{2+}) single crystal. The image contrast is better than that from an Agfa MD-30 imaging plate as can be seen in Fig. 1. The images were made using a 3 mm diameter Cu TEM grid (top Fig. 1) and a Mo tube operating at 50 kV and 30 mA. The read-out was via stimulating the entire plate with a red LED centered near 655 nm and the emitted light passed through a blue filter and the image was detected using a CCD camera.

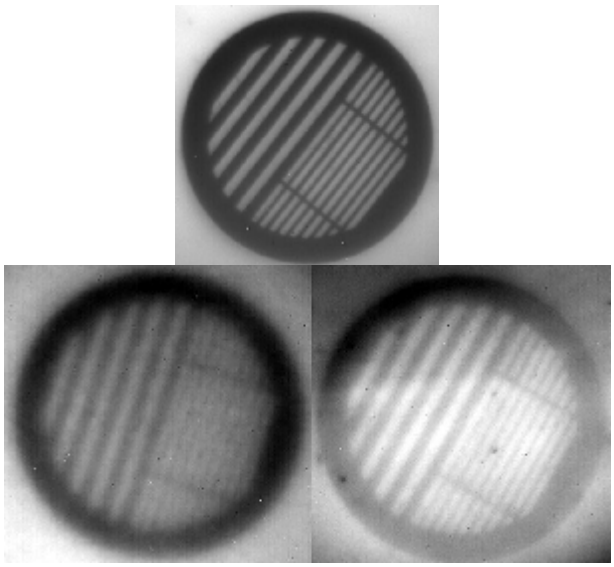

Figure 1*: Optical image (top), x-ray image using an Agfa MD-30 imaging plate (bottom left) and an x-ray image using one of our plates*

(bottom right) of a 3 mm diameter Cu TEM grid.

The bottom left image in Fig. 1 is from an Agfa MD-30 imaging plate and the bottom right image is from the glass-ceramic. The small (~40 μm) lines are more clearly resolved in the glass-ceramic but they are blurred in the Agfa MD-30 imaging plate. It should be noted that the Agfa MD-30 imaging plate has been optimized for a different readout method using a scanning laser spot.

An estimate of the ultimate spatial resolution was obtained by a point-by-point readout using a confocal micro-Raman spectrometer. The OSL emission spectra are shown in Fig. 2a for 10 μm step sizes across a gold mask edge. The integrated intensities are plotted in Fig. 2b. It can be seen that there is a well-defined edge for a step size of 10 μm.

The spatial resolution for radiation imaging plates is normally given in terms of the modulation transfer function (MTF), which can be obtained from the edge spread function (ESF). In Fig. 2 we show the ESF of Schweizer [6], $ESF(x)=\arctan(x/a)$, where x is the distance and a=0.0028 μm (dashed curve in Fig. 2b).

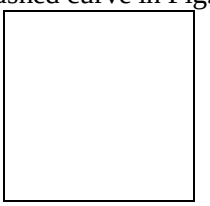

Figure 2*: OSL emission spectra at 10 mm steps across an x-ray image of a gold edge (top) and the integrated OSL intensity (bottom). The inset show the MTF.*

It can be shown that the corresponding $MTF(k)=\exp(-2pak)$, where k is in line pairs (lp) per mm. It is obtained by first differentiating the ESF, which for this ESF leads to the line spread function (LSF), $LSF(x)=a/(a^2+x^2)$. The Fourier transform of the LSF gives the MTF. For the Schweizer ESF it is apparent that the linewidth of the LSF and hence the spatial resolution is $2a$. It is easy to show that $2a \approx 0.5/k_{0.2}$, where $k_{0.2}$ is the value of k that leads to a MTF of 0.2.

We estimate from Fig. 2 that the spatial resolution of our glass-ceramic corresponds to ~90 lp/mm for a MTF of 0.2 and using a confocal microscope readout system, which is significantly greater than that obtained using the laser scanning method in commercial readout systems for the Agfa MD-30 imaging plate (~2.5 lp/mm at MTF=0.2).

Thermal neutron images [5,7] were taken of the perspex phantom in Fig. 3 (top) using a BAS2500 Imaging Plate readout scanner produced by Fujifilm. The corresponding Fujifilm BAS-ND image can be seen in Fig. 3 (bottom left) and the image from our first lithium-borate glass-ceramic thermal neutron imaging plate can be seen in Fig. 3 (bottom right). The thermal neutron images show the first and second steps starting from the left in Fig. 3 (top).

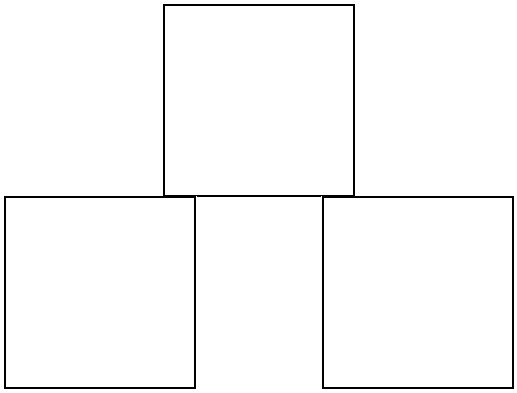

Figure 3*: Thermal neutron phantom (top), and the images obtained using the Fujifilm BAS-ND plate (bottom left) and our first imaging plate (bottom right).*

As mentioned earlier, the BAS-ND imaging plate uses a Gd thermal neutron converter where the cross-sections are 255000 barns for ^{157}Gd and 61000 for ^{155}Gd. Our imaging plates uses ^{6}Li and ^{10}B in the glass with cross-sections of 941 barns and 3838 barns respectively.

It can be seen in Fig. 3 that our first thermal neutron imaging plate had a lower spatial resolution than that obtainable using the Fujifilm BAS-ND imaging plate.

The spatial resolution was measured by plotting the 1D intensity across an edge of a thermal neutron image [5,7]. The resultant MTF was obtained by fitting the data to the ESF of Schweizer [6]

The spatial resolution for a MTF of 0.2 corresponds to 8.4 lp/mm for the Fujifilm plate and 2.8 lp/mm for our best plate. This gives a spatial resolution of ~60 μm for the Fujifilm plate and ~180 μm for our plate. The spatial resolution of our imaging plates is degraded by afterglow and we believe that it can be improved and exceed that of

the Fujifilm plate by choosing another phosphor, which is part of our current research program.

The relative conversion efficiency was estimated by comparing the intensity of the images after thermal neutron irradiation. We estimate that the CE of our thermal neutron imaging plate is ~145 % when compared with the BAS-ND imaging plate. Thus, even though the thermal neutron capture cross section is only ~8 % for our plate with ^{6}Li and ^{10}B when compared with the Fujifilm plate with ^{155}Gd and ^{157}Gd, we find that the CE is larger in our plate. This cannot be attributed to the different storage phosphors because BaFBr:Eu^{2+} is known to have a high CE when compared with $BaCl_2$:Eu^{2+}. It is likely that a large fraction of the conversion electron energy is not being transferred to the phosphor crystallites and light is also lost by scattering from the BaFBr:Eu^{2+} crystallites.

Another important consideration for thermal neutron imaging is the effect of residual radiation from neutron activation. This requires careful storage of the thermal neutron imaging plate. The most important activation for the Fujifilm BAS-ND plate occurs with the ^{79}Br and ^{81}Br nuclei because the radioactive decay includes γ-ray with penetrating 620 keV and 780 keV energies. There is also radioactive decay from ^{151}Eu but the decay products are short range β particles.

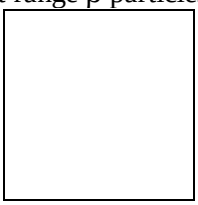

Figure 4*: Plot of the residual decay rate for the Fujifilm BAS-ND imaging plate (solid curve), our imaging plate (dashed) and the rate expected with 0.01 % Eu^{2+} (dotted curve). Inset: expanded curve.*

Most of the residual radiation in our imaging plate arises from ^{151}Eu because the ^{35}Cl halflife is very long (3.01×10^5 years). For comparative purposes we show the number of decays per second in Fig. 4 from the Fujifilm plate (solid curve) and our current plate with 0.5 % Eu^{2+} (dashed curve). We have recently found that our plates with 0.01 % Eu^{2+} are more sensitive than the first plates with 0.5 % Eu^{2+}. This will allow us to reduce the Eu^{2+} fraction and the residual decay rate (dotted curve) will be nearly an order of magnitude lower than that from the Fujifilm plate.

4. Conclusions

In conclusion, our x-ray imaging plates are nearly as sensitive as BaFBr(1000ppm Eu^{2+}) that is used in the commercial powdered phosphor imaging plates. The spatial resolution corresponds to 90 lp/mm. This is significantly better than that obtained from a Agfa MD-30 imaging plate used in medical imaging and optimized for a rapidly scanning laser spot read-out method. Our new thermal neutron imaging plate is more sensitive that the Fujifilm BAS-ND imaging plate and the residual radiation can be reduced by at least an order of magnitude. The spatial resolution is not as high as that found in the BAS-ND imaging plate, but we believe that we can achieve a superior spatial resolution with another nano-crystallite phosphor. This is part of our current research program.

5. Acknowledgement

We acknowledge funding from the New Zealand Foundation for Research Science and Technology. We thank P. Vontobel for assistance with the thermal neutron measurements.

6. References

[1] Edgar, A., Spaeth, J. M., Schweizer, S., Assmann, S., Newman, P. J., and MacFarlane, D. R., "Photostimulated luminescence in a rare earth-doped fluorobromozirconate glass ceramic", *Appl. Phys. Lett.*, 75:2386-2388. 1999.

[2] Edgar, A., Williams, G. V. M., Sagar, P. K. D., Secu, M., Schweizer, S., Spaeth, J. M., Hu, J., Newman, P. J., and MacFarlane, D. R., "A new fluorozirconate glass-ceramic x-ray storage phosphor", *J. Non-Cryst. Sol.*, 326&327:489-493, 2003.

[3] Edgar, A., Williams, G. V. M., Hamlin, J., Secu, M., Schweizer, S., and Spaeth, J. M., "New materials for glass-ceramic x-ray storage phosphors", *Current Applied Physics*, 4:193-196, 2004.

[4] Schweizer, S., Hobbs, L. W., Secu, M., Spaeth, J. M., Edgar, A., Williams, G. V. M., and Hamlin, J., "Photostimulated Luminescence from Fluorochlorozirconate Glass-Ceramics and the Effect of Crystallite Size", *J. Appl. Phys.*, 97:083522, 2005.

[5] Appleby, G. A., Edgar, A., Williams, G. V. M., and Vontobel, P., "Structure and neutron imaging characteristics of lithium borate - barium chloride glasses and glass-ceramics", *Nucl. Inst. Meth. A*, 564:424-430, 2006.

[6] Schweizer, S., "Physics and current understanding of x-ray storage phosphors", *Phys. Stat. Sol.*, 187:335-393, 2001.

[7] Appleby, G. A., "New Materials for Radiation Imaging", *PhD Thesis, Victoria University of Wellington, New Zealand*, 2006.